REPORT DOCUMENTATION PAGE

AFRL-SR-AR-TR-03-

0441

1. REPORT DATE (DD-MM-YYYY) 14-10-2003	2. REPORT TYPE Final Technical Report	3. DATES COVERED (From - To) 15 FEB 2000 - 14 FEB 2003

4. TITLE AND SUBTITLE	5a. CONTRACT NUMBER
Mechanism of ultrashort pulse laser injury to the RPE (Retinal Pigment Epithelium)	5b. GRANT NUMBER F49620-00-1-0179
	5c. PROGRAM ELEMENT NUMBER

6. AUTHOR(S) Charles P. Lin, PhD	5d. PROJECT NUMBER
	5e. TASK NUMBER
	5f. WORK UNIT NUMBER

7. PERFORMING ORGANIZATION NAME(S) AND ADDRESS(ES) Wellman Laboratories of Photomedicine Massachusetts General Hospital Harvard Medical School 50 Blossom Street Boston, MA 02114	8. PERFORMING ORGANIZATION REPORT NUMBER

9. SPONSORING / MONITORING AGENCY NAME(S) AND ADDRESS(ES) AFOSR	

20031104 011

12. DISTRIBUTION / AVAILABILITY STATEMENT

Approved for public release; distribution is unlimited.

13. SUPPLEMENTARY NOTES

14. ABSTRACT

Previous studies in our laboratory have established that microbubble formation inside the RPE cells is the damage mechanism for single exposures of short laser pulses from 100 fsec to ~1 μsec. In the current project, we investigated the mechanism for multiple laser pulse injury to RPE cells using a new pump-probe setup. We also investigated the expression of heat shock proteins as potential a marker of sublethal injury following short pulse laser exposure. Finally, we developed a slitlamp based light scattering system for monitoring laser-induced bubble formation in vivo.

15. SUBJECT TERMS
Laser injury, retina, retinal pigment epithelium, ultrashort pulses

16. SECURITY CLASSIFICATION OF:			17. LIMITATION OF ABSTRACT	18. NUMBER OF PAGES	19a. NAME OF RESPONSIBLE PERSON Charles P. Lin, PhD
a. REPORT	b. ABSTRACT	c. THIS PAGE	UL		19b. TELEPHONE NUMBER (include area code) 617-724-3957

Standard Form 298 (Rev. 8-98)
Prescribed by ANSI Std. Z39.18

Objectives

1. Investigate the mechanism for RPE injury from repetitive ultrashort pulse laser exposure. Test the hypothesis that threshold RPE damage requires cavitation bubble formation from a least one pulse in a train of multiple laser pulses. Experiments will be performed in RPE explants.

2. Develop pump-probe and photoacoustic methods to detect cavitation bubble formation in experimental rabbit eyes in vivo. The goal is to achieve sufficient sensitivity to detect theshold bubbles inside a single RPE cell, since minimum spot size lesions can involve damage to a single or very few RPE cells. Compare the threshold for RPE cavitation to the MVL threshold detected by standard ophthalmoscopic observation.

3. Study sublethal injury to the RPE following exposure to laser pulses at fluences below the threshold for cavitation and immediate cell death. Experiments will be performed with RPE explants.

a. Investigate damage to the cytoskeleton of the RPE cells using fluorescent probes that label actin bundles. Damage to the cytoskeleton below cavitation threshold, if found, will indicate the presence of sublethal thermal denaturation of the cellular proteins.

b. Investigate the induction of heat shock response in sublethally irradiated RPE cells.

c. Use long term culture of RPE explants and apoptotic assays to study delayed cell death.

FINAL TECHNICAL REPORT
AIR FORCE OFFICE OF SCIENTIFIC RESEARCH

1. Period covered: 15 FEB 2000 - 14 FEB 2003

2. Title of Proposal: Mechanism of ultrashort pulse laser injury to the RPE

3. Grant Number: F49620-00-1-0179

4. Name of Institution: Wellman Laboratories of Photomedicine
    Massachusetts General Hospital

5. Author of Report: Charles P. Lin, PhD
    Wellman Laboratories of Photomedicine
    Massachusetts General Hospital, BHX 630
    Harvard Medical School
    Boston, MA 02114

    voice: 617-724-3957
    fax: 617-724-2075
    email: lin@helix.mgh.harvard.edu

6. Manuscripts submitted/published

Brinkmann R, Hüttmann G, Rögener J, Roider J, Birngruber R, **Lin CP**. Origin of RPE-Cell Damage by pulsed laser irradiance in the ns to µs time regime. Lasers Surg Med, 27:451–464 (2000).

Lin CP. Selective Absorption by Melanin Granules and Selective Cell Targeting. In Fankhauser F and Kwasniewska S (Ed).: *Lasers in Ophthalmology - Surgical and Diagnostic Aspects,* Kugler Publication, The Hague, Netherlands (2003)

Roegener J, Brinkmann R, **Lin CP**. Pump-probe detection of laser-induced microbubble formation in retinal pigment epithelium cells. J. Biomed. Optics, (accepted).

7. Scientific personnel support by this grant

Charles P. Lin, PhD
Clemens Alt
Judith Runnels, PhD
Xunbin Wei, PhD
Alan Prossin

1

8. Inventions/Patents/Discoveries

A US patent application has been filed (MGH 1709.1) on selective photocoagulation of the RPE. The invention relates to methods of determining therapeutic end points and preventing collateral damage in laser surgical techniques. Specifically, we propose to monitor microbubble formation within the RPE as an endpoint for selective laser treatment for certain retinal disorders such as diabetic macular edema, central serous retinopathy, and drusen. This work is a direct spin-off of our AFOSR-sponsored research on the mechanism of short pulse laser injury to the retina.

Conventional laser photocoagulation has been extremely successful in treating a wide range of retinal disorders. However, standard treatment employs long laser pulses (~0.1 sec) that produce relatively large zones of thermal damage in the retina. As a result, blind spots are created at each site of laser treatment. We are developing a new laser treatment system (supported by NIH) to selectively target the RPE cells with short laser pulses, in order to minimizes collateral thermal damage to the adjacent neuroretina. The selective targeting approach preserves the photoreceptors overlying the RPE, thereby preserves the visual function over the laser treatment spot.

In conventional photocoagulation, the treatment endpoint is determined from the appearance of gray-white lesions resulting from thermal denaturation of the retina. In the selective approach, there is no visible clinical endpoint because the thermal lesion is not created. Damage to the RPE alone is not visible ophthalmoscopically. In order to determine when the treatment endpoint is reached (and to set proper laser dosimetry), we propose to use microbubble formation at the RPE as a clinical endpoint. From our short pulse laser injury studies, we have shown that threshold RPE damage is always accompanied by transient micobubble formation. These microbubbles, which expand and collapse on the timescale of 0.1 to 1 μsec, produce a transient increase in light scattering signal that can be detected by a sensitive photodetector. An instrument is currently under development for clinical applications.

9. Collaborators/Consultants

Ralf Brinkmann, Georg Schuele, Reginald Birngruber, Medical Laser Center, Lubeck, Germany. They are investigating the use of a hydrophone (optoacoustic detection) to monitor bubble formation in the RPE in vivo as an indication of laser-induced RPE cell damage. This method is complementary to the lightscattering approach used in our laboratory. The sensitivity of the two methods are being compared.

10. Honors or Awards.

Elected US Chair, Gordon Research Conference on Lasers in Medicine and Biology.

11. Key Findings/Results/Accomplishments:

Mechanism of RPE injury from multiple laser pulses

The aim of this project is to test the hypothesis that threshold RPE damage requires intracellular bubble formation from a least one pulse in a train of multiple laser pulses. Previous studies in our laboratory have established that microbubble formation inside the RPE cells is the damage mechanism for single exposures of short laser pulses from 100 fsec to ~1 μsec. As the rate of energy deposition exceeds the rate of thermal relaxation, the energy becomes confined to the absorbing structures – the melanin granules – within the RPE layer. These pigment microparticles form intracellular hot spots and initiate microscopic cavitation bubbles that expand and collapse on the timescale of 0.1 – 1 μsec [1-3]. The mechanical actions associated with microbubble expansion and implosion imparts damage to cells [2-5].

Previous studies have used a fast time-resolved imaging technique to visualize the transient microbubbles [1-3]. In this method, a laser pulse was applied to heat the particles and a second laser pulse, delayed in time relative to the first, was used to illuminate the sample for stroboscopic image capture. This method is difficult to implement for looking at multiple pulse effects. We have developed a simple pump-probe setup to detect microbubble formation within the RPE. In this method, bubble formation is detected as a transient increase in the probe beam backscattering signal during the lifetime of the bubble.

Nd:YAG
532nm, 12ns

Nd:YAG
532nm, cw

CCD Camera

APD

Diode Laser
830nm

200 micron
Pinhole

100mm PCX

50mm PCX

Beam
chopper

80mm PCX

400mm
Achromat

Dichroic
mirrors

1mm
Pinhole

200mm
PCX

Mirror with
Hole in the center

Ar+ 488nm

Dichroic
mirror

20x objective
Infinity, NA .42

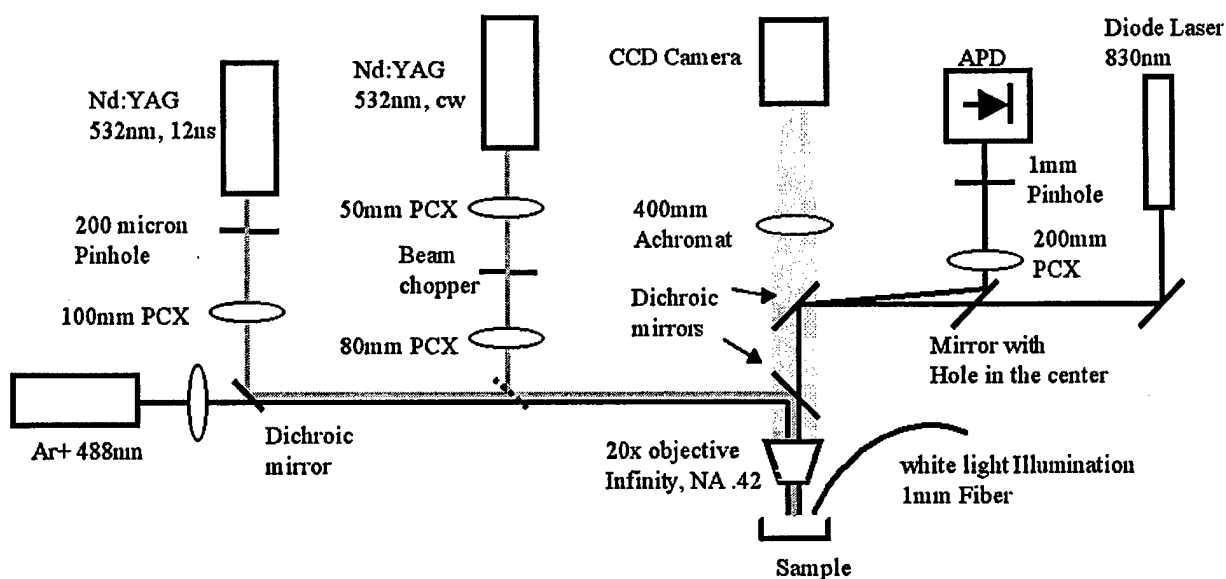white light Illumination
1mm Fiber

Sample

Figure 1 is a schematic diagram of the pump-probe setup. A 20x objective (Mitutoyo, NA=0.42, 25 mm working distance) was used to image the cells onto a CCD camera (Figure 1). The spatial resolution of the setup was approximately 1 µm. A frequency doubled, Nd:YAG Laser (Continuum, SEO 1-2-3, λ=532 nm, 6 mm beam) was used for 12 ns irradiation. A 200 µm section from the center of the beam was imaged onto the sample to give a flat top image of 20 µm diameter. The intensity variations at the sample due to hot spots in the beam were below 15%, as determined by imaging a fluorescent target within the area of irradiation after making sure that the fluorescence intensity was linear. A continous wave (cw) frequency doubled Nd:YAG Laser (Verdi, Coherent, λ=532 nm) was used together with a rotating wheel chopper to produce 6 µsec pulses at 500Hz. The gaussian shaped spot has a FWHM of 16 µm at the sample and the average power was 75 mW. To probe the bubble formation the collimated beam of a diode laser (SF830S-18, Microlaser Systems, 830 nm, 1.5x2 mm beam diameter) was focused onto the RPE cell to

produce a spot size of 7x10 μm (FWHM) with a maximum power of 1 mW at the sample. For each experiment, the RPE cells were examined through the microscope and the sample stage was positioned so that only one cell (10-15 μm diameter) was in the center of the irradiation laser spot. The probe beam, which was slightly smaller that an REP cell, was always placed on the cell in the center. The probe beam was switched on for less than 10 μs and switched off (1% power) 2-4 μs after the end of the 532 nm laser pulse. Backscattering of the probe beam was detected in a confocal geometry and also slightly off the optical axis to reduce specular reflection and scattering from the optical system and from tissue layers other than the RPE. The detector used was an avalanche photodiode (Hamamatsu C-5460) with a built-in high speed amplifier with 10 MHz bandwidth.

Porcine eyes of approx. 20mm diameter were prepared 0 to 4 hours after enucleation. After dissecting the eyes at the equatorial position, the anterior portion and the vitreous were removed. A sheet of 1 cm^2 was cut out of the posterior region of the eye and the sample was suspended in 0.9% saline solution. After 20 minutes the retina could be easily peeled off. The sample was flattened at the edges using a plastic ring. The RPE was covered with diluted CalceinAM (Molecular Probes) 1 μg/ml in PBS or Dulbecco's modified eagle medium (Gibco). A cover slip was applied on top. After 20 Minutes viable cells accumulated enough fluorescent Calcein to be distinguished from dead cells by fluorescence microscopy. Calcein fluorescence was excited at 488 nm and detected with a 540 nm long pass filter. One fluorescence image was taken before and a second 15-30 minutes after irradiation. Non-fluorescing cells where classified as dead. For 12 ns experiments the sample temperature was

20°C. This was done to ensure that the measurement condition was the same as that used in previous stroboscopic imaging experiments. Since the temperature required for bubble formation at the surface of the melanosom has been determined to be about 150°C [4], a background temperature of 20 or 35°C was not expected to make a significant difference in the threshold. On the other hand, for 6 µs pulses the sample was kept at a more physiologic temperature of 35°C in order not to bias our measurement against a potential thermal contribution to the cell death mechanism. The thresholds were calculated using a PC program for probit analyses [6] after Finney [7].

Results - nsec pulses

For 12 ns pulses 4 samples from 4 different eyes were used on which a total of 117 spots were irradiated at different fluences (40 controls with the Nd:YAG beam only, 77 with the Nd:YAG plus probe beam). Each irradiation spot was approximately the size of a single RPE cell. Results are listed in Table 1. The threshold for cavitation bubble detection was the same as the threshold for RPE cell death measured by Calcein fluorescence.

	F_{th} (mJ/cm^2)	F_{LL} (mJ/cm^2)	F_{UL} (mJ/cm^2)	slope	# cells
cell death	71	66	75	17	77
cavitation	71	67	75	16	77
control	71	66	81	14	40

Table 1. 12 nsec single pulse thresholds for cavitation and cell death

An example of the backscattered probe beam signal at 90 mJ/cm^2 (1.27x threshold) is shown in Figure 2. The diode laser was switched on at 0.2 μs and switched off at 3.4 μs to minimize sample heating. The pedestal between 0.2 and 3.4 μs is due to backscattering from the RPE tissue. The Nd:YAG laser was fired at 1.2 μs, which caused a transient increase in the backscattering of the probe beam from a single RPE cell. The bubble lifetime was about 500 nsec. Both the transient signal and the lifetime increase with increasing radiant exposure, rising up to 2% of the probe beam intensity at several times threshold, which is the maximum expected for a planar air/water interface.
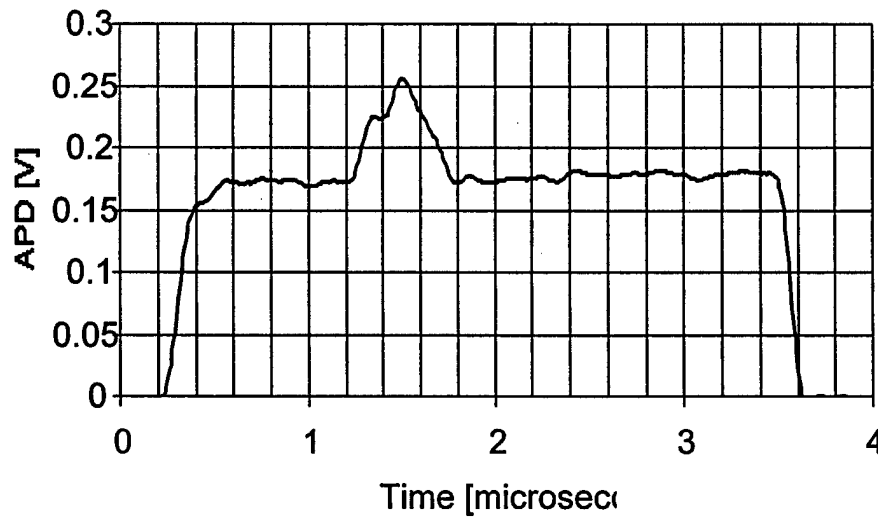

Figure 2. Backscattered probe beam signal from a 12 nsec laser pulse (90mJ/cm^2). The laser pulse was switched on at 1.2 μs.

Close to threshold the signals were more difficult to discern. In some events the reflected intensity showed a small increase at the time of irradiation and remained constant for the duration of the probe pulse (several μsec). Events were classified as positive if the signal increase was greater than 5% of the background during the first

500 ns after the irradiation. Out of the total 77 cells, there were 7 false negative and 6 false positive events within 20% of the ED_{50} threshold, but on average the threshold for bubble detection was the same as the threshold for cell killing (Table 1). At 20% above threshold no cell survived and all cells showed true positive bubble signals.

Results - μsec pulses

For 6 μs irradiation, 4 samples from 4 different eyes were used. A total of 241 cells were irradiated. For each sample, 1, 10, and 100 exposures were applied (at different spots). For single pulses the threshold for bubble detection was 11% higher than the threshold for cell killing. For 10 and 100 pulses the thresholds for bubble detection were 25% and 16 % higher, respectively (Table 2). All thresholds decreased with increasing number of pulses.

	# Pulses	F_{th} (mJ/cm$_2$)	F_{LL} (mJ/cm$_2$)	F_{UL} (mJ/cm$_2$)	slope	# cells
cell death	1	412	386	436	14	105
cavitation	1	456	425	484	16	105
cell death	10	306	264	355	12	33
cavitation	10	381	320	445	11	33
cell death	100	322	281	359	8	70
cavitation	100	374	335	413	9	70
control	100	286	246	338	14	30

Table 2. 6 μsec thresholds for cavitation and cell death.

An example of the oscilloscope trace is shown in Figure 3. At threshold, both the signal amplitude and the bubble lifetime for microsecond laser-induced bubbles were significantly greater than for nanosecond laser-induced bubbles. The lifetime was almost always longer than a microsecond (with only one exception out of ~100 measurements). Cavitation always started before the end of the Nd:YAG laser pulse.
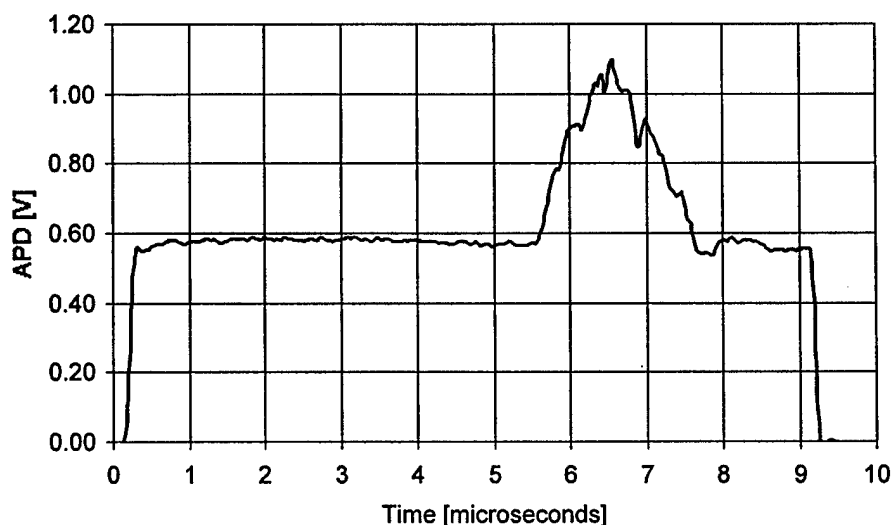

Figure 3. Backscattered probe beam signal from a 6 μs laser pulse (350 mJ/cm^2). The probe beam was switched on at the same time as the irradiation pulse and lasted for 10 μs.

For multiple pulse exposures near threshold, a bubble was often detected in only one or a few pulses (at random) out of the whole sequence (Figure 4). Whenever, a bubble was detected, even if one occurred only once in the pulse train, the cell was killed. Above threshold, cavitation appeared during each pulse. At threshold, cavitation appeared at arbitrary pulses (Figure 4), sometimes followed by cavitation within the next pulses, sometimes only at one pulse within the series. The ED_{50} for 100 pulses with probe beam is close to the control (without probe beam).
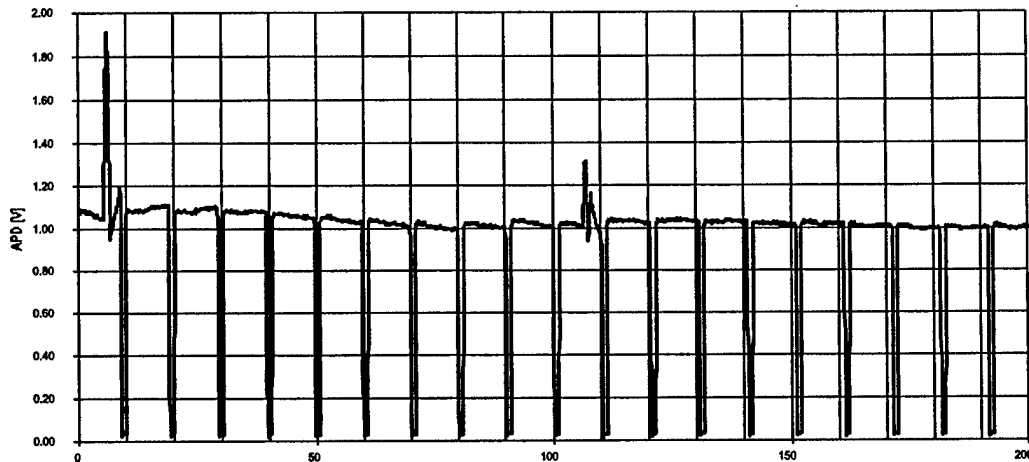
Figure 4. Backscattered probe beam signal from repetitive 6 μs laser pulses (425 mJ/cm^2). Only the first 15 pulses out of a train of 100 pulses are shown in the graph. The probe beam is switched on for 10 μs during and after irradiation. The 2 ms interpulse periods are not shown. Cavitation occurs on pulse 1 and 11.

Significance

For 12 ns pulses the threshold for cell death is the same as for bubble detection using the probe beam method. This is in agreement with Kelly et al who showed that cell death coincided with intracellular bubble formation detected by the stroboscopic imaging method [1-3]. Although the thresholds were the same (on average), some false positive and some false negative events were observed (6 false positive and 7 false negative events were detected out of 77 cells within 20% of the ED_{50} threshold). A false positive event means a bubble was detected but the cell survived; a false negative event means bubble was not detected but the cell lost viability. Previous studies have shown, using cultured endothelial cells (EC) containing ingested pigment particles, that that it is possible (but rare) to create small bubbles in the EC

without killing the cells [5]. For heavily pigmented cells such as the RPE, which contain numerous pigment granules in each cell, it is expected that irradiation of the particles will produce many bubbles simultaneously within each cell. These bubbles can coalesce to form larger bubbles and most likely cause cell death. Near threshold, however, it is possible that very small bubbles are formed around just one or a few melanin granules, giving rise to a bubble signal without killing cells. However, these false positive events were unexpected and the origins of these signals need to be investigated further. False negative signals, on the other hand, could mean either a) some cells die without cavitation, or b) cell cavitated but a bubble was not detected. We favor the latter interpretation because the size of the bubble can be much smaller than the size of the RPE cell (the lifetime of the smallest bubble detected was about 200 ns, corresponding to a bubble diameter of about 2 μm). It is possible that bubbles occurring on the edges of the cell were not detected because the probe beam size (FWHM 7μm x 10μm, elliptical) was slightly smaller than the RPE cell (10-15 μm) and also smaller than the excitation spot size (20 μm). The probe beam could be expanded to cover a larger area, but then one has to compromise the sensitivity at the center of the cell (for the same probe laser power).

Occasionally near threshold, the probe beam signal showed a small increase at the time of the laser pulse and remained constant for the duration of the probe pulse (several μsec). Most likely this signal is due to change in backscattering of the RPE cell as a result of spatial rearrangement or alteration of the melanosomes following the laser pulse. Since these events happened rarely and very close to the threshold with no detectable bubbles, formation of long-lasting bubbles is not likely to be the

origin of the signal. For a cavitation bubble to give rise to stable gas bubbles after its collapse, the initial cavity has to be large enough (hundreds of micrometers), with a lifetime long enough (at least tens of microseconds) to allow the dissolved gas to escape into the cavity by "rectified diffusion". The cavitation produced in the RPE cells in our experiments are much too small to produce such stable bubbles (at least none that are visible under the microscope).

With 6μs pulse duration, which is longer than the thermal relaxation time of a 1 μm melanosome (~1 μs), there is significant heat diffusion away from the particles during the laser pulse. Consequently the thresholds for cell death (412 mJ/cm^2) and for bubble detection (456 mJ/cm^2) are both higher than for 12 nsec pulses. However, this increase in threshold is not as dramatic as the values predicted for bubble formation around a single, isolated melanosome [4]. Mutual heating among the closely-spaced melanosome particles within the RPE cell can be a significant cause for the temperature increase during the microsecond laser pulses, leading to higher temperatures than an isolated melanosome would reach [4]. Mutual heating is insignificant for 12 nsec pulses because there is much less heat diffusion outside the particles.

In general, the threshold bubble signals from 6 μs laser exposures were stronger and had longer lifetimes (> 1 μsec) than the threshold bubble signals from 12 nsec laser pulses. A lifetime of 1 μsec corresponds to a spherical bubble diameter of ~10 μm. Larger bubbles are expected for μsec laser pulses because the threshold radiant exposure is higher (a larger volume of surrounding fluid is heated as a result of heat diffusion away from the particle) than for nsec pulses.

The ED$_{50}$ values for cell death were comparable with and without the probe beam; indicating that the probe beam did not significantly affect the temperature of the sample. This was shown for 100 pulses and therefore should be true for 1 or 10 pulses. The radiant exposure (~14 mJ/cm^2) produced by probe beam (1 mW, 10 μsec long pulse in a 7 μm x 10 μm spot) was more than a factor of 20 below the threshold for cell death. In addition, the melanosome absorption at the wavelength of the probe beam (830 nm) was lower than the absorption at 532 nm. Consequently, the probe beam by itself was not expected to have a significant heating effect on the RPE.

The difference between the ED$_{50}$ for cell death and for bubble detection can mean the existence of a damage mechanism that does not involve bubble formation. However, this difference is small (11%) and bubble formation is not ruled out as the mechanism for microsecond laser-induced RPE cell death. Further improvement in bubble detection sensitivity will be necessary to resolve this issue. It is unlikely that strong shock waves are produced without bubble formation because the pulse duration is much longer than the stress confinement time in our experiments. The stress confinement time, or the time for an acoustic wave to travel across the particle, is less than 1 nsec for a 1 μm particle.

The threshold declines with multiple pulse exposures. Previous studies have found an empirical relationship between damage threshold and the number of pulses, N, that generally follows the $N^{-1/4}$ power law for thermal damage processes. However, if the damage mechanism is not thermal but is mediated by bubble formation, then it is still possible for the threshold to decline with the number of pulses but not with the $N^{-1/4}$ dependence. An important finding in this study is that a

single cavitation event during a long train of pulses is sufficient to kill the cell. Hence with increasing number of pulses the probability increases for bubble formation in one of the pulses. This is the likely reason for the threshold reduction.

Detecting laser-induced bubble formation in RPE cells in vivo.

Based on the success of the pump-probe detection method described above, we progressed to develop an in vivo system for monitoring laser-induced bubble formation in the RPE of living eyes. The goal is to achieve sufficient sensitivity to detect theshold bubbles inside a single RPE cell, since minimum spot size lesions can involve damage to a single or very few RPE cells.

The scattering phase function for a growing bubble was calculated, based on Mie's scattering theory, to determine the fraction of an incident probe beam that is backscattered at the target tissue:

$$f_{Mie}(\theta) = \frac{S_1 S_1^* + S_2 S_2^*}{2\pi \int\limits_0^\pi \left[S_1 S_1^* + S_2 S_2^* \right] \sin\theta d\theta},$$

where

$$S_1(\theta) = \sum_{n=1}^{\infty} \frac{2n+1}{n(n+1)} \left\{ a_n \frac{P_n^1(\cos\theta)}{\sin\theta} + b_n \frac{d}{d\theta} P_n^1(\cos\theta) \right\},$$

$$S_2(\theta) = \sum_{n=1}^{\infty} \frac{2n+1}{n(n+1)} \left\{ b_n \frac{P_n^1(\cos\theta)}{\sin\theta} + a_n \frac{d}{d\theta} P_n^1(\cos\theta) \right\},$$

$P_n^1(\cos\theta)$ are the associated Legendre functions, a_n and b_n are the coefficients of the Mie series (which depend on the wavelength, λ, the size of the scatterer, and the relative refractive index n). In the simulations, the following optical properties of the

growing, non-absorbing bubble were used: $\lambda= 532$ nm, $n=1/1.33$, and the size of the bubble was varied from 1 μm to 5 μm.

To estimate the fraction of incident light backscattered within the field of view of our detector, the following formula was used:

$$\frac{S_{backscat}}{S_{total}} \cdot \frac{A_{bubble}}{A_{probe}} \cdot Q_{scat}$$

where A_{bubble} and A_{probe} are the cross sectional area of the bubble and the probe beam, respectively. Q_{scat} is the scattering coefficient, defined as the ratio of the scattering cross section to the geometric cross section. S_{total} is the total area under the $f_{Mie}(\square)$ curve and $S_{backscat}$ the area under $f_{Mie}(\square)$ within the specified angles. Low numerical aperture (NA of 0.1 and 0.05) detection was assumed to more closely approximate conditions in the human (or rabbit) eye.

Figure 5 shows a polar plot of the scattering phase function for a growing bubble (1-5 μm). Figure 6 shows the fraction of light incident on the bubble that is backscattered and collected within the solid angle corresponding to NA=0.1 and 0.05 (f/5 and f/10, respectively). At $\lambda=532$ nm, approximately 0.001% of a 10 μm laser beam incident on a 5 μm bubble can be sampled at the detector. These results point to the need for a very sensitive detection scheme for bubble detection in vivo because of the small fraction of the probe beam that is backscattered.
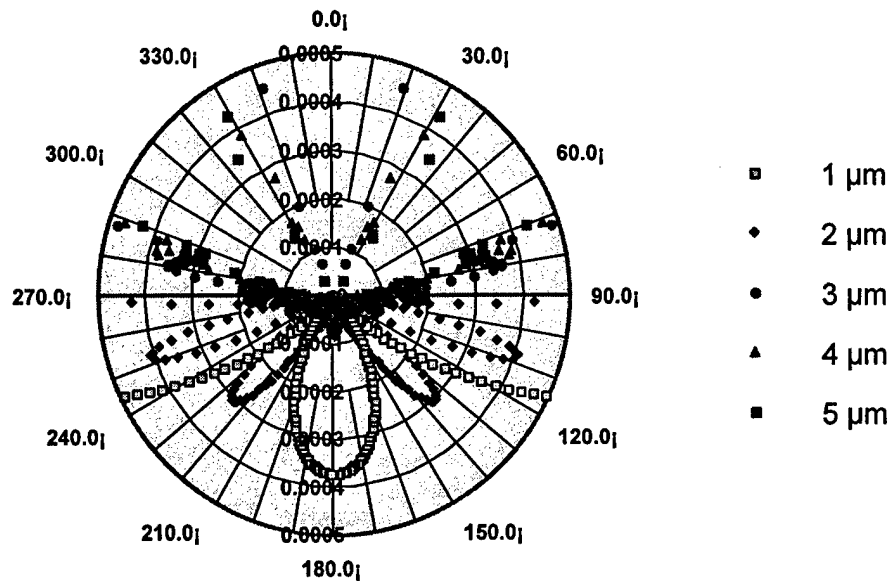
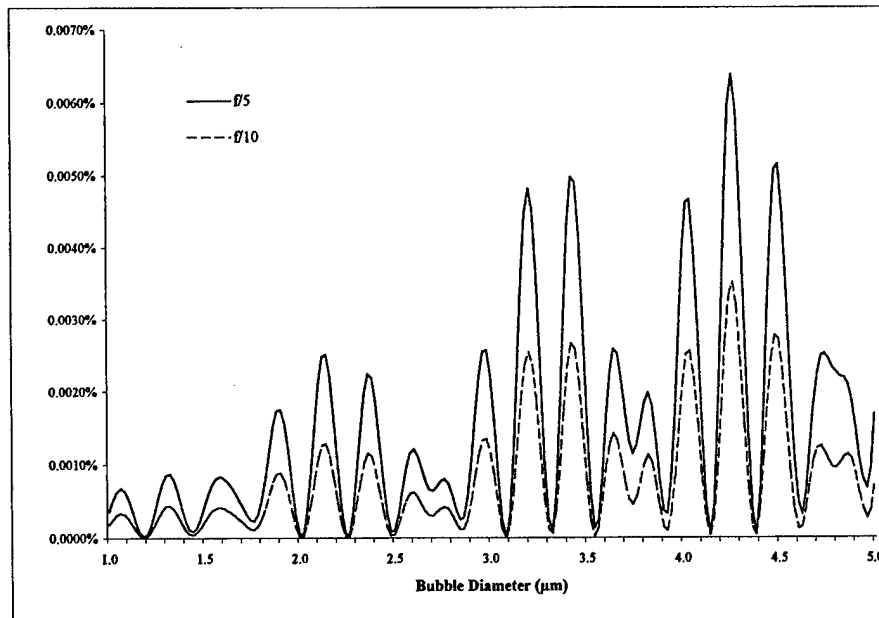Figure 5. Mie scattering phase function for a 1 - 5 μm bubble.

Figure 6. Fraction of back-scattered light from a growing bubbled, detected in a solid angle corresponding to f/5 and f/10.

A slitlamp-based confocal light scattering detection system has been assembled as shown in Figure 7. The confocal pinholes is needed to reject photons backscattered from other structures (e.g. cornea) within the eye. The detector is a silicon avalanche photodiode (Hamamatsue C5460) with a 10 MHz bandwidth, which is needed to detect the rapidly growing and collapsing bubble. Although we have not yet succeeded in detecting bubbles from single RPE cells in vivo, we are continuing to improve the sensitivity of the detection system in order to achieve this goal.

QuickTime™ and a TIFF (Uncompressed) decompressor are needed to see this picture.

Figure 7. Slit-lamp based bubble detection setup.

<u>Sublethal cellular injury following exposure to laser pulses at fluences below the threshold for cavitation and immediate cell death</u>.

Preliminary studies were performed in cultured endothelial cells labeled with 0.83 μm iron oxide particles. The particles were ingested by the endothelial cells and sequestered in endosomes/lysosomes. When irradiated by short laser pulses, intracellular cavitation bubbles were produced around the particles, similar to the bubble formation process induced around the melanin particles in the RPE. The pigmentation was controlled by varying the particle/cell ratio during incubation. We used this model system to investigate the effect of short pulse laser irradiation at sublethal fluences (i.e. below the fluence for cavitation and cell killing). Specifically, we investigate Hsp27 and Hsp70 production following laser irradiation. Hsp27 and Hsp70 are two members of the heat shock protein (Hsp) family that was originally identified on the basis of their expression after cellular exposure to high temperatures [8]. These proteins can protect against cell death (apoptosis) induced by hyperthermia, oxidative stress, etc.

Production of Hsp27 and Hsp70 in bovine aorta endothelial cells incubated with 1, 10, or 100 particles per cell and irradiated with nanosecond laser pulses (532 nm, 0.2-0.4 J/cm^2) was determined by western blot analysis. We found the levels of Hsp27 and Hsp70 expression to be unaltered for up to 4 days following laser exposure. These preliminary results need to be confirmed in RPE cells.

Literature cited

1. C. P. Lin and M. W. Kelly, "Cavitation and acoustic emission around laser-heated microparticles," Appl. Phys. Lett, vol. 72, pp 2800-2802 (1998).

2. W.W. Kelly and C. P. Lin. "Microcavitation and cell injury in RPE cells following short-pulsed laser irradiation". Proc SPIE 2975:174–179 (1997).

3. C. P. Lin, M. W. Kelly, S. A. Sibayan, M. A. Latina, R. R. Anderson. "Selective Cell Killing by Microparticle Absorption of Pulsed Laser Radiation". IEEE J Select Topics Quant Electron., 5:963-968 (1999).

4. Brinkmann R, Hüttmann G, Rögener J, Roider J, Birngruber R, Lin CP. Origin of RPE-Cell Damage by pulsed laser irradiance in the ns to μs time regime. Lasers Surg Med, 27:451–464 (2000).

5. D. Leszczynski, C. M. Pitsillides, R. R. Anderson, C. P. Lin. "Laser-Beam-Triggered Microcavitation: A Novel Method for Selective Cell Destruction". Radiation Research, 156:399-407 (2001).

6. C. P. Cain , G. D. Noojin, L. Manning. "A Comparison of Various Probit Methods for Analyzing Yes/No Data on a Log Scale". US Air Force Armstrong Laboratory, AL/OE-TR-1996-0102 (1996).

7. D. J. Finney. "Probit Analysis" 3rd ed. London:Camebridge University Press (1971).

8. Strunnikova N, Baffi J, Gonzalez A, Silk W, Cousins SW, Csaky KG. Regulated heat shock protein 27 expression in human retinal pigment epithelium. Invest Ophthalmol Vis Sci. 42:2130-8 (2001).